JOURNAL OF MOLECULAR SPECTROSCOPY 170, 59–74 (1995)

High-Resolution Fourier Transform Infrared Emission Spectra of Barium Monofluoride

B. GUO, K. Q. ZHANG, AND P. F. BERNATH

Centre for Molecular Beams and Laser Chemistry, Department of Chemistry, University of Waterloo, Waterloo, Ontario, Canada N2L 3G1

The high-resolution infrared emission spectra of gas-phase barium monofluoride have been observed by Fourier transform spectrometry. Vibration–rotation bands were analyzed for the three most abundant isotopomers (^{138}BaF, from 1–0 to 12–11; ^{137}BaF, from 1–0 to 5–4; ^{136}BaF, from 1–0 to 4–3) of the ground $X^2\Sigma^+$ state. The Dunham coefficients, Y_{lm}, have been derived for all three isotopomers by fitting about 1750 lines for ^{138}BaF, about 270 lines for ^{137}BaF, and about 70 lines for ^{136}BaF to the traditional Dunham model. In addition, the mass-reduced Dunham constants, U_{lm}, have been calculated from a global least-squares fit. © 1995 Academic Press, Inc.

INTRODUCTION

Studies of the barium monofluoride molecule can be traced back into the past century to work by Mitscherlich (*1*). By employing flames and arcs as the main sources of emission, George (*2*), Datta (*3*), Johnson (*4*), and Nevin (*5*) reported the first series of band spectra of BaF in the 1930s. About the same time, the absorption spectra of BaF were reported by Walters and Barratt (*6*) and by Jenkins and Harvey (*7*). However, these observations were confined mostly to the visible region, and the resolution was usually limited by the congestion of atomic and molecular lines, as well impurity bands. Barrow *et al.* (*8*) performed the first rotational analysis of one band of each of five electronic systems of BaF in 1967. The thermally excited emission spectra of BaF were studied by Singh and Mohan in 1971 (*9*).

The microwave spectrum of the ground state of BaF, $X^2\Sigma^+$, was measured by Ryzlewicz and Törring (*10*). In their work, 12 rotational transitions with vibrational quantum numbers up to 4 for the ^{138}BaF isotopomer and three rotational lines with $v = 0$ for the ^{136}BaF isotopomer were measured. In another paper, Ryzlewicz *et al.* (*11*) also measured the hyperfine structure for the ^{137}BaF isotopomer. Ip *et al.* (*12*) reported the optical–optical double resonance spectrum of BaF. Recently, Effantin *et al.* (*13*) have studied the low-lying electronic transitions by both thermal emission and laser-excited fluorescence recorded with a Fourier transform spectrometer. Together they have assigned about 6470 rotational lines to 24 bands of 10 systems and obtained the effective molecular constants for the seven low-lying electronic states below 30 000 cm^{-1}. Subsequent work by Bernard *et al.* (*14*) and Effantin *et al.* (*15*) has extended the studies of the band systems to higher vibrational levels and new electronic states. Very recently, the Rydberg states of BaF were studied by Jakubek and Field (see (*16*, *17*)), and an accurate ionization potential of 38 742 cm^{-1} was obtained.

As part of the systematic investigation of the alkaline earth monofluorides in our laboratory, we report here our high-resolution Fourier transform infrared emission

0022-2852/95 $6.00

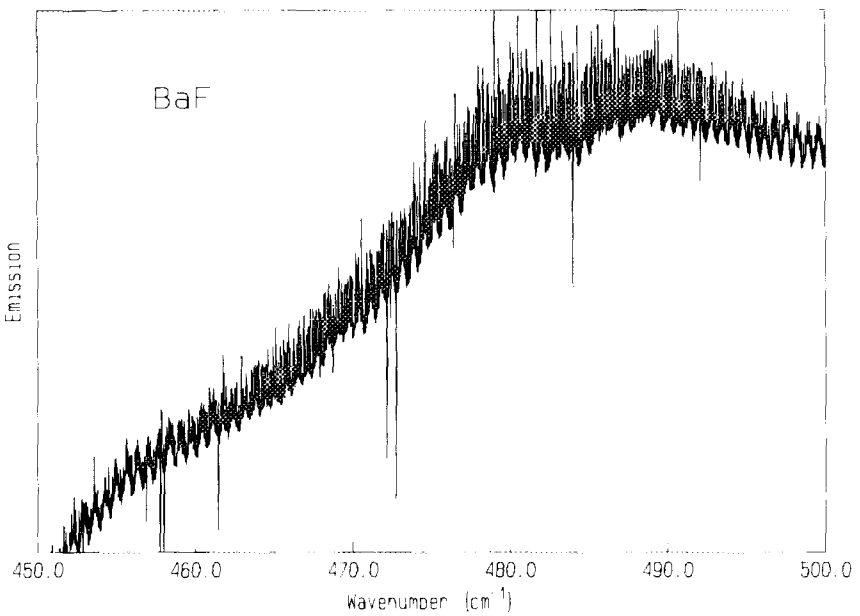

FIG. 1. An overview of the vibration–rotation emission spectrum of BaF.

spectrum of BaF in the ground $X\,^2\Sigma^+$ state. Three isotopomers, all occurring in natural abundance (^{138}Ba, 71.70%; ^{137}Ba, 11.23%; ^{136}Ba, 7.85%) (*18*) were analyzed and rotational constants were determined. The Dunham coefficients, Y_{lm}, have been derived

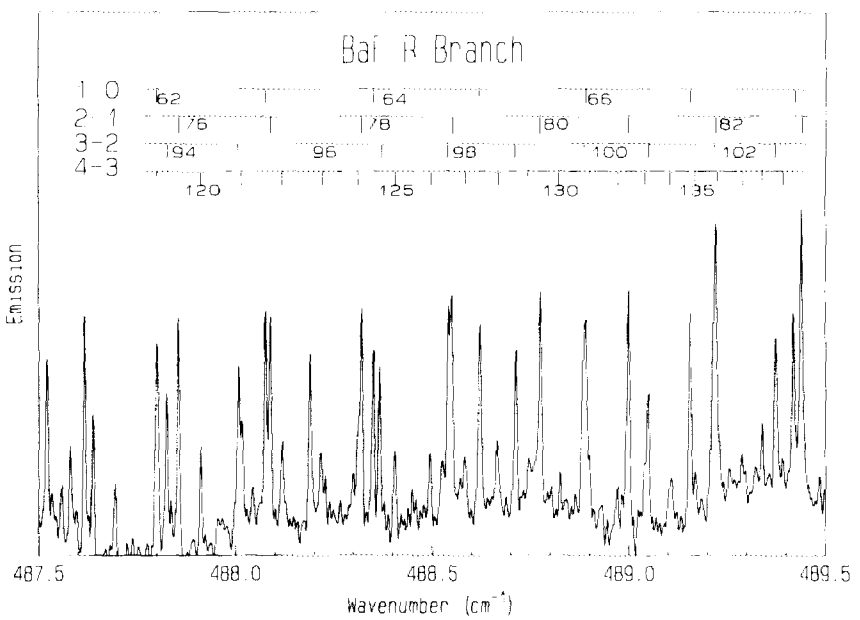

FIG. 2. A portion of the spectrum showing some *R*-branch lines of BaF.

for all three isotopomers. In addition, the mass-reduced Dunham constants, U_{lm}, are also derived from a global least-squares fit.

EXPERIMENTAL DETAILS

The high-resolution infrared emission spectrum of barium monofluoride was recorded with the Bruker IFS 120 HR Fourier transform spectrometer at University of

TABLE Ia

Line Positions of ^{138}BaF in cm^{-1}

N'	N''	ν_{obs}	10^4O-C	N'	N''	ν_{obs}	10^4O-C	N'	N''	ν_{obs}	10^4O-C
		0 - 0 band*		34	35	449.2772	3	53	52	485.1953	-12
6	5	2.5912166	-0.0020	33	34	449.7860	7	54	53	485.4965	2
7	6	3.0230192	0.0007	32	33	450.2908	-7	55	54	485.7934	-1
8	7	3.4547904	-0.0007	31	32	450.7948	-6	56	55	486.0882	1
21	20	9.0629837	-0.0007	30	31	451.2989	16	57	56	486.3805	3
22	21	9.4938563	-0.0016	29	30	451.7973	5	58	57	486.6696	-0
		1 - 0 band		28	29	452.2914	-29	59	58	486.9563	-3
100	101	411.1111	2	27	28	452.7888	-7	60	59	487.2408	-1
99	100	411.7515	-27	26	27	453.2825	-1	61	60	487.5228	2
98	99	412.3961	5	25	26	453.7732	-1	62	61	487.8029	12
96	97	413.6708	-18	24	25	454.2613	-7	63	62	488.0779	-2
94	95	414.9425	8	23	24	454.7487	4	64	63	488.3519	-0
92	93	416.2033	0	22	23	455.2334	9	65	64	488.6234	2
90	91	417.4587	17	21	22	455.7146	2	66	65	488.8913	-4
88	89	418.7008	-21	20	21	456.1942	0	67	66	489.1575	-2
87	88	419.3216	-13	19	20	456.6725	9	68	67	489.4210	-0
85	86	420.5569	-2	18	19	457.1481	13	69	68	489.6822	5
84	85	421.1697	-14	17	18	457.6203	5	70	69	489.9396	-1
83	84	421.7833	-0	16	17	458.0914	8	71	70	490.1951	1
82	83	422.3933	-2	15	16	458.5572	-19	72	71	490.4476	-2
80	81	423.6073	-5	14	15	459.0263	9	73	72	490.6953	-26
79	80	424.2095	-25	13	14	459.4904	11	74	73	490.9452	-0
78	79	424.8135	-7	12	13	459.9506	-5	75	74	491.1900	1
77	78	425.4138	-6	11	12	460.4125	20	76	75	491.4319	0
76	77	426.0124	-2	11	10	470.3418	-1	77	76	491.6720	7
75	76	426.6075	-12	12	11	470.7475	19	78	77	491.9077	-3
74	75	427.2017	-12	13	12	471.1467	-2	79	78	492.1421	1
73	74	427.7944	-8	14	13	471.5452	-7	80	79	492.3738	6
72	73	428.3840	-13	15	14	471.9400	-24	81	80	492.6013	-4
71	72	428.9750	16	16	15	472.3348	-17	82	81	492.8269	-7
70	71	429.5595	-0	17	16	472.7269	-14	83	82	493.0516	8
69	70	430.1447	11	18	17	473.1185	9	84	83	493.2719	8
68	69	430.7262	5	19	18	473.5034	-12	85	84	493.4887	-1
67	68	431.3071	15	20	19	473.8907	16	86	85	493.7039	0
66	67	431.8844	8	21	20	474.2723	10	87	86	493.9163	2
65	66	432.4589	-6	22	21	474.6508	-2	88	87	494.1261	5
64	65	433.0332	-2	23	22	475.0274	-9	89	88	494.3320	-3
63	64	433.6051	-1	24	23	475.4056	25	90	89	494.5363	0
62	63	434.1754	4	25	24	475.7767	11	91	90	494.7372	-3
61	62	434.7426	0	26	25	476.1456	1	92	91	494.9358	-3
60	61	435.3084	1	27	26	476.5120	-11	93	92	495.1321	4
59	60	435.8716	-3	28	27	476.8781	-0	94	93	495.3251	3
58	59	436.4340	7	29	28	477.2410	2	95	94	495.5144	-6
57	58	436.9926	-2	30	29	477.6028	18	96	95	495.7015	-9
56	57	437.5489	-12	31	30	477.9591	4	97	96	495.8866	-3
55	56	438.1063	10	32	31	478.3160	20	98	97	496.0689	2
54	55	438.6565	-20	33	32	478.6678	10	99	98	496.2475	-3
53	54	439.2091	-5	35	34	479.3645	-4	100	99	496.4241	0
52	53	439.7588	3	36	35	479.7119	16	101	100	496.5978	3
51	52	440.3056	2	37	36	480.0521	-10	102	101	496.7680	-1
50	51	440.8505	3	38	37	480.3955	21	103	102	496.9352	-7
49	50	441.3929	1	39	38	480.7307	-7	104	103	497.1007	-1
48	49	441.9345	11	40	39	481.0655	-12	105	104	497.2631	1
47	48	442.4713	-5	41	40	481.3997	1	106	105	497.4220	-3
46	47	443.0078	-4	42	41	481.7308	9	107	106	497.5795	7
45	46	443.5429	6	43	42	482.0573	-4	108	107	497.7322	-2
44	45	444.0739	-5	44	43	482.3836	6	109	108	497.8829	-3
43	44	444.6062	20	45	44	482.7057	-1	110	109	498.0310	-2
42	43	445.1323	3	46	45	483.0264	4	111	110	498.1763	1
41	42	445.6568	-9	47	46	483.3456	19	112	111	498.3182	-3
40	41	446.1812	-0	48	47	483.6589	0	113	112	498.4567	-11
39	40	446.7029	4	49	48	483.9709	-6	114	113	498.5942	-1
37	38	447.7389	2	50	49	484.2810	-6	115	114	498.7276	-3
36	37	448.2553	17	51	50	484.5891	0	116	115	498.8588	2
35	36	448.7660	-3	52	51	484.8928	-12	117	116	498.9867	2

TABLE Ia—*Continued*

N'	N"	ν_{obs}	10^3O-C	N'	N"	ν_{obs}	10^3O-C	N'	N"	ν_{obs}	10^3O-C
118	117	499.1106	-8	51	52	436.7865	-4	34	33	475.2963	-6
119	118	499.2339	5	50	51	437.3293	0	35	34	475.6425	1
120	119	499.3523	-2	49	50	437.8700	5	36	35	475.9857	1
121	120	499.4690	3	48	49	438.4079	3	37	36	476.3267	6
122	121	499.5812	-9	47	48	438.9439	3	38	37	476.6643	0
123	122	499.6923	-1	46	47	439.4766	-8	39	38	476.9999	0
124	123	499.8003	4	45	46	440.0095	3	40	39	477.3330	0
125	124	499.9053	8	44	45	440.5393	5	41	40	477.6632	-4
126	125	500.0069	9	43	44	441.0666	3	42	41	477.9904	-13
127	126	500.1056	10	42	43	441.5919	3	43	42	478.3160	-13
128	127	500.2004	1	41	42	442.1153	4	44	43	478.6402	-1
129	128	500.2928	-3	40	41	442.6364	4	45	44	478.9610	2
130	129	500.3825	-4	39	40	443.1555	6	46	45	479.2804	15
131	130	500.4685	-12	38	39	443.6717	1	47	46	479.5942	-2
132	131	500.5534	-1	37	38	444.1867	4	48	47	479.9069	-4
133	132	500.6350	6	36	37	444.6988	-0	49	48	480.2185	8
134	133	500.7123	-0	35	36	445.2095	4	50	49	480.5270	15
135	134	500.7880	8	34	35	445.7172	-0	51	50	480.8308	-0
136	135	500.8597	6	33	34	446.2236	5	52	51	481.1335	-1
137	136	500.9283	3	32	33	446.7272	3	53	52	481.4342	5
138	137	500.9940	0	31	32	447.2271	-15	54	53	481.7308	-5
139	138	501.0582	13	30	31	447.7283	3	55	54	482.0262	-1
140	139	501.1158	-9	29	30	448.2258	6	56	55	482.3190	2
141	140	501.1749	13	28	29	448.7196	-6	58	57	482.8961	2
142	141	501.2271	-3	27	28	449.2146	15	59	58	483.1805	-1
143	142	501.2778	-5	26	27	449.7042	4	60	59	483.4631	4
		1 - 1 band*		25	26	450.1929	7	61	60	483.7422	0
6	5	2.5772667	0.0035	24	25	450.6786	3	62	61	484.0187	-4
7	6	3.0067435	0.0001	23	24	451.1619	-5	63	62	484.2929	-4
21	20	9.0141466	0.0002	22	23	451.6443	1	64	63	484.5647	-2
		2 - 1 band		21	22	452.1233	-4	65	64	484.8337	-2
90	91	414.0362	-2	20	21	452.6001	-10	66	65	485.1009	5
87	88	415.8949	3	19	20	453.0766	4	67	66	485.3642	1
85	86	417.1224	-12	18	19	453.5493	2	68	67	485.6278	26
84	85	417.7353	2	17	18	454.0193	-4	69	68	485.8835	-3
83	84	418.3449	1	16	17	454.4881	0	70	69	486.1405	9
82	83	418.9501	-23	15	16	454.9543	1	71	70	486.3927	-1
80	81	420.1611	-6	14	15	455.4189	8	72	71	486.6435	2
79	80	420.7637	4	13	14	455.8789	-8	73	72	486.8906	-6
78	79	421.3624	-6	12	13	456.3388	-4	74	73	487.1360	-4
77	78	421.9611	5	11	12	456.7962	0	75	74	487.3786	-3
76	77	422.5562	-1	10	11	457.2508	-2	76	75	487.6186	-2
75	76	423.1492	-7	9	10	457.7030	-6	77	76	487.8564	4
74	75	423.7402	-13	8	9	458.1539	-0	78	77	488.0903	-2
73	74	424.3313	1	9	8	465.8640	-2	79	78	488.3224	1
72	73	424.9197	8	10	9	466.2713	10	80	79	488.5516	2
71	72	425.5079	34	11	10	466.6734	-7	81	80	488.7774	-4
70	71	426.0889	9	12	11	467.0755	-0	82	81	489.0003	-12
69	70	426.6693	-4	16	15	468.6573	-0	83	82	489.2227	2
68	69	427.2497	5	17	16	469.0469	2	84	83	489.4410	3
67	68	427.8272	5	18	17	469.4344	6	85	84	489.6566	3
66	67	428.4019	-3	19	18	469.8183	-2	86	85	489.8693	2
65	66	428.9750	-6	20	19	470.1989	-18	87	86	490.0790	-2
64	65	429.5464	-5	21	20	470.5808	2	88	87	490.2848	-18
63	64	430.1167	4	22	21	470.9578	-2	89	88	490.4912	1
62	63	430.6839	3	23	22	471.3333	3	90	89	490.6953	22
61	62	431.2487	-1	24	23	471.7053	-3	91	90	490.8921	-1
60	61	431.8135	16	25	24	472.0752	-6	92	91	491.0869	-17
59	60	432.3734	3	26	25	472.4444	9	93	92	491.2819	-3
58	59	432.9321	0	27	26	472.8087	0	94	93	491.4725	-5
57	58	433.4887	-3	28	27	473.1711	-4	95	94	491.6608	-2
56	57	434.0461	22	29	28	473.5316	-4	96	95	491.8463	-1
55	56	434.5975	8	30	29	473.8907	9	97	96	492.0284	-5
54	55	435.1493	19	31	30	474.2458	6	98	97	492.2086	1
53	54	435.6959	-1	32	31	474.5973	-10	99	98	492.3851	-4
52	53	436.2419	-6	33	32	474.9484	-4	100	99	492.5587	-9

Waterloo. The spectrum was obtained with a liquid-helium-cooled Si:B detector and a KBr beamsplitter at a resolution of 0.007 cm^{-1}. The spectra bandpass was limited to ~400–760 cm^{-1} by a cold filter for the upper wavenumber limit and by the beamsplitter cut off for the lower limit.

The experimental setup was similar to that described in an earlier paper (*19*). Gas-phase barium monofluoride molecules were produced in a tube furnace by gradually heating a mixture of barium difluoride and barium metal. The barium metal pieces and barium difluoride powder were contained in two carbon boats lying inside

TABLE Ia—*Continued*

N'	N"	ν_{obs}	10^4O-C	N'	N"	ν_{obs}	10^4O-C	N'	N"	ν_{obs}	10^4O-C
101	100	492.7306	-4	70	71	422.6333	-25	15	14	464.6077	3
102	101	492.8990	-4	69	70	423.2154	5	16	15	464.9964	-6
103	102	493.0655	4	68	69	423.7931	12	17	16	465.3829	-13
104	103	493.2281	1	67	68	424.3673	4	18	17	465.7695	5
105	104	493.3884	3	66	67	424.9401	2	19	18	466.1518	4
106	105	493.5447	-6	64	65	426.0805	8	20	19	466.5274	-40
107	106	493.7007	10	63	64	426.6465	0	21	20	466.9087	-2
108	107	493.8510	-4	62	63	427.2120	7	22	21	467.2829	-12
109	108	494.0002	2	61	62	427.7738	-3	23	22	467.6567	-1
110	109	494.1454	-5	60	61	428.3349	2	24	23	468.0272	1
111	110	494.2882	-7	59	60	428.8941	8	25	24	468.3927	-23
112	111	494.4285	-5	58	59	429.4494	-5	26	25	468.7599	-6
113	112	494.5664	1	57	58	430.0048	4	27	26	469.1227	-7
114	113	494.7006	-1	56	57	430.5561	-7	28	27	469.4845	5
115	114	494.8325	2	55	56	431.1071	0	29	28	469.8419	-2
116	115	494.9609	-1	54	55	431.6550	-3	30	29	470.1989	11
117	116	495.0862	-6	53	54	432.2018	3	31	30	470.5518	8
118	117	495.2097	1	52	53	432.7458	2	32	31	470.9025	7
119	118	495.3305	9	51	52	433.2877	1	33	32	471.2499	-1
120	119	495.4467	-0	50	51	433.8267	-7	34	33	471.5957	-2
121	120	495.5600	-9	49	50	434.3652	0	35	34	471.9400	8
122	121	495.6709	-13	48	49	434.9006	-3	36	35	472.2797	-3
123	122	495.7798	-8	47	48	435.4353	9	37	36	472.6181	-3
124	123	495.8866	7	46	47	435.9658	0	38	37	472.9545	3
125	124	495.9879	-5	45	46	436.4955	4	39	38	473.2870	-6
126	125	496.0877	-3	44	45	437.0227	4	40	39	473.6186	1
127	126	496.1832	-14	43	44	437.5489	15	41	40	473.9470	1
128	127	496.2789	6	42	43	438.0704	1	42	41	474.2723	-5
129	128	496.3691	1	41	42	438.5909	-3	43	42	474.5973	12
130	129	496.4573	4	40	41	439.1098	1	44	43	474.9165	-4
131	130	496.5418	1	39	40	439.6268	5	45	44	475.2358	6
133	132	496.7017	-7	38	39	440.1405	-2	46	45	475.5506	-4
134	133	496.7781	-2	37	38	440.6516	-13	47	46	475.8638	-5
135	134	496.8526	14	36	37	441.1638	9	48	47	476.1748	-2
136	135	496.9214	3	35	36	441.6707	-2	49	48	476.4836	5
137	136	496.9891	10	34	35	442.1763	-2	50	49	476.7859	-28
138	137	497.0519	-1	33	34	442.6810	9	51	50	477.0920	2
139	138	497.1128	-2	32	33	443.1816	2	52	51	477.3922	-1
140	139	497.1708	-1	31	32	443.6806	-1	53	52	477.6905	2
141	140	497.2267	9	30	31	444.1774	-3	54	53	477.9841	-16
142	141	497.2789	12	29	30	444.6732	7	55	54	478.2785	0
143	142	497.3266	-0	28	29	445.1660	8	56	55	478.5686	-1
144	143	497.3726	2	27	28	445.6568	12	57	56	478.8561	-3
145	144	497.4155	3	26	27	446.1432	-7	58	57	479.1415	1
146	145	497.4551	1	25	26	446.6304	5	59	58	479.4238	-2
147	146	497.4911	-6	24	25	447.1131	-7	60	59	479.7050	12
		2 - 2 band*		23	24	447.5957	3	61	60	479.9814	3
6	5	2.5633299	0.0176	22	23	448.0752	4	62	61	480.2554	-4
7	6	2.9904822	0.0007	21	22	448.5520	-1	63	62	480.5270	-9
		3 - 2 band		20	21	449.0275	5	64	63	480.7975	2
89	90	411.2553	14	19	20	449.4989	-8	65	64	481.0655	13
86	87	413.0988	4	18	19	449.9718	15	66	65	481.3281	-4
85	86	413.7078	-16	17	18	450.4383	-2	67	66	481.5897	-3
84	85	414.3174	-10	16	17	450.9042	-3	68	67	481.8493	4
83	84	414.9257	3	15	16	451.3705	22	69	68	482.1050	-3
82	83	415.5296	-9	14	15	451.8300	1	70	69	482.3586	-3
81	82	416.1344	9	13	14	452.2914	22	71	70	482.6097	-3
80	81	416.7354	8	12	13	452.7463	1	72	71	482.8584	1
79	80	417.3338	1	11	12	453.2004	-5	73	72	483.1037	-3
78	79	417.9320	12	10	11	453.6521	-12	74	73	483.3456	-15
77	78	418.5264	4	9	10	454.1040	4	75	74	483.5876	1
75	76	419.7099	-4	10	9	462.6237	-2	76	75	483.8266	15
74	75	420.2990	-3	11	10	463.0266	13	77	76	484.0610	8
73	74	420.8842	-23	12	11	463.4230	-15	78	77	484.2929	4
72	73	421.4701	-15	13	12	463.8209	-2	79	78	484.5217	-5
71	72	422.0554	6	14	13	464.2156	1	80	79	484.7493	2

a half-meter-long carbon liner. The carbon liner was placed in the center of a 1.2-m-long and 5-cm-diameter alumina tube which was sealed with two KRS-5 windows at both ends. The tube was heated by a commercial furnace. The ends of the alumina tube were water cooled in order to prevent metal vapor condensation on the window. After the sample was loaded, the alumina tube was pumped and heated to about 150°C overnight in order to remove the water from inside the tube. About 10 Torr of argon gas was introduced into the tube before the temperature was increased. The spectral region between 400 and 750 cm^{-1} was monitored as the temperature in-

TABLE Ia—*Continued*

N'	N"	ν_{obs}	10^4O-C	N'	N"	ν_{obs}	10^4O-C	N'	N"	ν_{obs}	10^4O-C
81	80	484.9731	-3	68	69	420.3543	4	8	7	458.1930	19
82	81	485.1953	3	67	68	420.9263	-1	9	8	458.5963	13
83	82	485.4130	-8	66	67	421.4966	-3	10	9	458.9967	2
84	83	485.6278	-21	65	66	422.0665	13	11	10	459.3947	-10
85	84	485.8439	5	64	65	422.6333	17	12	11	459.7916	-9
86	85	486.0544	3	63	64	423.1969	10	13	12	460.1882	13
87	86	486.2618	-2	62	63	423.7582	-1	14	13	460.5792	3
88	87	486.4671	-2	61	62	424.3190	5	15	14	460.9688	1
89	88	486.6696	-1	60	61	424.8763	-4	16	15	461.3550	-10
90	89	486.8689	-6	59	60	425.4321	-7	17	16	461.7392	-16
91	90	487.0662	-3	58	59	425.9871	2	18	17	462.1237	4
92	91	487.2606	-2	57	58	426.5393	5	19	18	462.5035	0
93	92	487.4522	-1	56	57	427.0884	-4	20	19	462.8810	-2
94	93	487.6404	-6	55	56	427.6358	-8	21	20	463.2561	-3
95	94	487.8268	-1	54	55	428.1821	-3	22	21	463.6286	-7
96	95	488.0103	2	53	54	428.7259	-2	23	22	463.9985	-13
97	96	488.1908	3	52	53	429.2683	6	24	23	464.3686	8
98	97	488.3681	0	51	52	429.8066	-6	25	24	464.7343	8
99	98	488.5430	1	50	51	430.3449	2	26	25	465.0959	-7
100	99	488.7145	-5	49	50	430.8805	6	27	26	465.4570	-4
101	100	488.8830	-12	48	49	431.4138	6	28	27	465.8172	15
102	101	489.0509	3	47	48	431.9440	-3	29	28	466.1718	3
103	102	489.2139	-4	46	47	432.4725	-8	30	29	466.5274	25
104	103	489.3760	9	45	46	433.0013	12	31	30	466.8770	12
105	104	489.5322	-8	44	45	433.5235	-14	32	31	467.2245	2
106	105	489.6885	3	43	44	434.0461	-15	33	32	467.5703	-1
107	106	489.8400	-5	42	43	434.5687	7	34	33	467.9126	-13
108	107	489.9902	2	41	42	435.0866	2	35	34	468.2556	6
109	108	490.1353	-14	40	41	435.6043	17	36	35	468.5931	-6
110	109	490.2792	-12	39	40	436.1176	9	37	36	468.9297	-1
111	110	490.4207	-7	38	39	436.6281	-6	38	37	469.2632	-2
112	111	490.5596	1	37	38	437.1368	-17	39	38	469.5942	-3
113	112	490.6953	6	36	37	437.6456	-5	40	39	469.9231	-1
114	113	490.8268	-3	35	36	438.1518	2	41	40	470.2491	-2
115	114	490.9572	6	34	35	438.6565	16	42	41	470.5720	-10
117	116	491.2067	-3	33	34	439.1559	-1	43	42	470.8919	-22
118	117	491.3278	-0	32	33	439.6547	-4	44	43	471.2123	-4
119	118	491.4447	-11	31	32	440.1522	4	45	44	471.5286	-2
120	119	491.5610	2	30	31	440.6449	-15	46	45	471.8425	2
121	120	491.6720	-9	29	30	441.1383	-6	47	46	472.1529	-5
122	121	491.7826	4	28	29	441.6304	12	48	47	472.4615	-4
123	122	491.8894	9	27	28	442.1153	-19	49	48	472.7685	7
124	123	491.9923	4	26	27	442.6022	-9	50	49	473.0715	2
125	124	492.0932	8	25	26	443.0869	2	51	50	473.3737	16
126	125	492.1901	1	24	25	443.5681	-1	52	51	473.6706	1
127	126	492.2860	14	23	24	444.0479	5	53	52	473.9659	-3
128	127	492.3738	-24	22	23	444.5243	-2	54	53	474.2599	5
129	128	492.4661	11	21	22	444.9999	6	55	54	474.5501	1
131	130	492.6333	-3	20	21	445.4717	-3	56	55	474.8381	0
132	131	492.7133	-2	19	20	445.9423	0	57	56	475.1235	-1
133	132	492.7905	2	18	19	446.4106	2	58	57	475.4056	-8
134	133	492.8645	3	17	18	446.8773	10	59	58	475.6869	2
135	134	492.9345	-7	16	17	447.3392	-9	60	59	475.9646	1
136	135	493.0038	6	15	16	447.8011	-4	61	60	476.2394	-2
		3 - 3 band*		14	15	448.2630	24	62	61	476.5120	-1
7	6	2.9742360	-0.0011	13	14	448.7196	21	64	63	477.0491	-2
		4 - 3 band		12	13	449.1721	-1	65	64	477.3137	-3
77	78	415.1102	-6	11	12	449.6251	5	66	65	477.5760	0
76	77	415.7006	-8	10	11	450.0751	3	67	66	477.8355	1
75	76	416.2898	-1	9	10	450.5232	6	68	67	478.0922	0
74	75	416.8775	10	8	9	450.9685	3	69	68	478.3462	-2
73	74	417.4587	-24	7	8	451.4121	6	70	69	478.5979	0
72	73	418.0427	-10	6	7	451.8527	2	71	70	478.8465	-2
71	72	418.6240	-3	5	6	452.2914	1	72	71	479.0914	-16
70	71	419.2037	9	6	5	457.3765	3	73	72	479.3356	-10
69	70	419.7789	-5	7	6	457.7850	3	74	73	479.5772	-3

creased. When the temperature reached about 1450°C, the emission of BaF started to appear. The temperature was then increased to 1500°C, and the spectrum was taken with 130 scans coadded. Figure 1 shows an overview of the spectrum of barium monofluoride.

ANALYSIS AND RESULTS

The spectral analysis program PC-DECOMP, developed by J. W. Brault, was used for the spectral line measurement. Using this program, the spectral line profiles were

TABLE Ia—*Continued*

N'	N''	ν_{obs}	10^4O-C	N'	N''	ν_{obs}	10^4O-C	N'	N''	ν_{obs}	10^4O-C
75	74	479.8158	1	73	74	414.0539	-16	14	13	456.9618	2
76	75	480.0521	8	71	72	415.2144	9	15	14	457.3490	1
77	76	480.2839	-3	70	71	415.7914	18	16	15	457.7336	-4
78	77	480.5145	1	69	70	416.3636	1	17	16	458.1160	-6
79	78	480.7431	12	68	69	416.9349	-6	18	17	458.4970	2
80	79	480.9678	10	67	68	417.5061	7	19	18	458.8747	1
81	80	481.1883	-6	66	67	418.0747	12	20	19	459.2496	-5
82	81	481.4091	8	65	66	418.6392	-1	21	20	459.6230	-1
83	82	481.6264	13	64	65	419.2037	5	22	21	459.9927	-10
84	83	481.8395	4	63	64	419.7640	-10	23	22	460.3627	7
85	84	482.0496	-9	62	63	420.3275	28	24	23	460.7279	1
86	85	482.2593	2	61	62	420.8842	17	25	24	461.0916	5
87	86	482.4649	0	60	61	421.4367	-15	27	26	461.8109	4
88	87	482.6679	-1	59	60	421.9928	10	28	27	462.1670	4
89	88	482.8684	-0	58	59	422.5433	-1	29	28	462.5175	-26
90	89	483.0662	1	57	58	423.0929	0	30	29	462.8718	5
91	90	483.2608	-3	56	57	423.6389	-15	31	30	463.2206	6
92	91	483.4534	2	55	56	424.1865	7	32	31	463.5660	-3
93	92	483.6425	-1	54	55	424.7276	-14	33	32	463.9106	5
94	93	483.8266	-27	53	54	425.2713	11	34	33	464.2512	-3
95	94	484.0115	-17	52	53	425.8096	2	35	34	464.5919	16
96	95	484.1935	-8	51	52	426.3465	1	36	35	464.9281	14
97	96	484.3718	-9	50	51	426.8810	-4	37	36	465.2599	-7
98	97	484.5486	4	49	50	427.4144	3	38	37	465.5915	-5
99	98	484.7213	3	48	49	427.9451	2	39	38	465.9220	11
100	99	484.8928	18	47	48	428.4743	7	40	39	466.2488	14
101	100	485.0571	-11	46	47	428.9998	-3	41	40	466.5742	29
102	101	485.2233	7	45	46	429.5240	-6	42	41	466.8929	1
103	102	485.3834	-8	44	45	430.0469	0	43	42	467.2118	1
104	103	485.5430	0	43	44	430.5661	-9	44	43	467.5284	3
105	104	485.6988	-1	42	43	431.0836	-15	45	44	467.8423	4
106	105	485.8526	6	41	42	431.5996	-14	46	45	468.1536	2
107	106	486.0024	1	40	41	432.1151	3	47	46	468.4623	1
108	107	486.1490	-8	39	40	432.6282	18	48	47	468.7684	-1
109	108	486.2933	-11	38	39	433.1354	-6	49	48	469.0736	13
110	109	486.4359	-4	37	38	433.6421	-12	50	49	469.3732	-3
111	110	486.5756	4	36	37	434.1478	-7	51	50	469.6727	5
112	111	486.7117	3	35	36	434.6519	3	52	51	469.9682	-2
113	112	486.8439	-7	34	35	435.1493	-32	53	52	470.2621	2
114	113	486.9749	-0	33	34	435.6518	6	54	53	470.5518	-11
115	114	487.1019	-5	32	33	436.1466	-12	55	54	470.8416	3
116	115	487.2276	5	31	32	436.6427	6	56	55	471.1273	1
117	116	487.3483	-6	30	31	437.1368	24	57	56	471.4101	-5
118	117	487.4659	-19	29	30	437.6243	-1	58	57	471.6913	0
119	118	487.5831	-7	28	29	438.1148	26	59	58	471.9686	-8
120	119	487.6971	2	27	28	438.5992	13	60	59	472.2449	-0
122	121	487.9139	-5	26	27	439.0814	-1	61	60	472.5173	-6
123	122	488.0195	7	25	26	439.5633	6	62	61	472.7899	17
124	123	488.1206	4	24	25	440.0421	4	63	62	473.0560	-0
125	124	488.2195	7	23	24	440.5174	-13	64	63	473.3206	-6
126	125	488.3138	-6	22	23	440.9931	-2	65	64	473.5832	-5
127	126	488.4069	-2	21	22	441.4659	2	66	65	473.8436	0
128	127	488.4963	-6	20	21	441.9345	-15	67	66	474.1012	3
129	128	488.5853	16	19	20	442.4040	0	68	67	474.3552	-4
130	129	488.6673	-3	18	19	442.8697	0	69	68	474.6084	9
131	130	488.7487	2	16	17	443.7939	-6	70	69	474.8570	1
132	131	488.8278	13	15	16	444.2536	-0	71	70	475.1038	1
133	132	488.9018	3	14	15	444.7111	6	72	71	475.3473	-5
		4 - 4 band*		13	14	445.1660	11	73	72	475.5894	1
7	6	2.9580063	0.0045	12	13	445.6176	3	74	73	475.8285	4
		5 - 4 band		11	12	446.0684	11	75	74	476.0647	5
79	80	410.5335	2	10	11	446.5138	-13	76	75	476.2962	-14
78	79	411.1252	-1	10	9	455.3869	-13	77	76	476.5281	-4
77	78	411.7159	6	11	10	455.7850	-1	78	77	476.7559	-6
76	77	412.3034	0	12	11	456.1796	0	79	78	476.9823	3
74	75	413.4726	-9	13	12	456.5716	-2	80	79	477.2050	4

fitted to Voigt lineshape functions. The signal-to-noise ratio for the strongest lines in the spectrum was about 10:1. The HF molecule was present in the spectra as an impurity. The measured spectral lines were calibrated with the HF lines using line positions taken from the literature (*20*). The precision of the line position measurement is better than ± 0.0007 cm^{-1} for most of the strong and unblended lines. However, many of the weaker lines and the blended features were determined only to a lesser precision of about ± 0.001 cm^{-1}.

The fundamental band and the first few hot bands of ^{138}BaF were easily identified by using an interactive color Loomis–Wood program because the band heads were

TABLE Ia—*Continued*

N'	N"	ν_{obs}	10^4O-C	N'	N"	ν_{obs}	10^4O-C	N'	N"	ν_{obs}	10^4O-C
81	80	477.4255	8	49	50	423.9672	-6	40	39	462.5916	4
82	81	477.6418	-3	48	49	424.4962	1	41	40	462.9124	-5
83	82	477.8555	-12	47	48	425.0225	3	42	41	463.2321	-0
84	83	478.0676	-11	46	47	425.5473	10	43	42	463.5484	-5
85	84	478.2785	6	45	46	426.0687	4	44	43	463.8631	0
86	85	478.4844	1	44	45	426.5886	5	45	44	464.1741	-6
87	86	478.6885	3	43	44	427.1048	-10	46	45	464.4832	-8
88	87	478.8891	-2	42	43	427.6211	-4	47	46	464.7909	3
90	89	479.2804	-27	41	42	428.1356	7	48	47	465.0959	11
91	90	479.4753	-7	40	41	428.6456	-7	49	48	465.3979	15
92	91	479.6661	1	39	40	429.1564	9	50	49	465.6958	4
93	92	479.8535	1	38	39	429.6614	-12	51	50	465.9919	0
94	93	480.0392	12	37	38	430.1686	11	52	51	466.2859	1
95	94	480.2185	-14	36	37	430.6698	-5	53	52	466.5742	-31
97	96	480.5750	-2	35	36	431.1723	14	54	53	466.8662	1
98	97	480.7508	22	34	35	431.6690	-4	55	54	467.1517	-7
99	98	480.9193	-2	33	34	432.1645	-12	56	55	467.4355	-7
100	99	481.0879	6	32	33	432.6603	5	57	56	467.7174	1
101	100	481.2530	5	31	32	433.1534	16	58	57	467.9957	-2
103	102	481.5735	-9	30	31	433.6421	4	59	58	468.2696	-23
104	103	481.7308	-3	29	30	434.1301	8	60	59	468.5449	-3
105	104	481.8852	2	28	29	434.6166	19	61	60	468.8155	-6
106	105	482.0366	4	27	28	435.0975	-5	62	61	469.0847	4
107	106	482.1847	3	26	27	435.5788	-3	63	62	469.3493	-6
108	107	482.3295	-4	25	26	436.0561	-18	64	63	469.6124	-6
109	108	482.4729	4	24	25	436.5349	3	65	64	469.8740	7
111	110	482.7481	-11	23	24	437.0095	4	66	65	470.1309	-2
112	111	482.8833	-0	22	23	437.4804	-10	67	66	470.3843	-20
113	112	483.0152	6	21	22	437.9496	-18	68	67	470.6383	-5
114	113	483.1433	3	20	21	438.4199	7	69	68	470.8919	31
115	114	483.2684	-1	19	20	438.8840	-9	70	69	471.1350	-11
116	115	483.3943	32	18	19	439.3484	2	71	70	471.3800	-6
117	116	483.5113	4	17	18	439.8090	-4	72	71	471.6218	-9
118	117	483.6287	9	16	17	440.2669	-15	73	72	471.8614	-6
119	118	483.7422	4	15	16	440.7205	-46	74	73	472.0990	4
120	119	483.8543	14	13	14	441.6304	-14	75	74	472.3348	21
121	120	483.9606	-5	11	12	442.5300	6	76	75	472.5641	0
123	122	484.1695	6	9	10	443.4189	9	77	76	472.7899	-28
124	123	484.2672	-12	8	9	443.8583	-6	78	77	473.0191	4
126	125	484.4587	1	12	11	452.5861	-1	79	78	473.2419	-1
127	126	484.5486	-7	13	12	452.9751	-8	80	79	473.4617	-10
128	127	484.6370	-1	14	13	453.3656	22	81	80	473.6811	4
129	128	484.7213	-6	15	14	453.7476	-10	82	81	473.8992	32
130	129	484.8051	12	17	16	454.5113	-4	83	82	474.1095	9
131	130	484.8830	2	18	17	454.8905	8	84	83	474.3183	-2
132	131	484.9585	-4	19	18	455.2658	6	85	84	474.5254	-2
133	132	485.0312	-7	20	19	455.6404	20	86	85	474.7309	9
134	133	485.1009	-12	21	20	456.0104	12	87	86	474.9315	-2
135	134	485.1713	21	22	21	456.3773	-3	88	87	475.1310	3
		6 - 5 band		23	22	456.7438	3	89	88	475.3269	-1
70	71	412.3961	2	24	23	457.1070	-1	90	89	475.5209	3
69	70	412.9666	-7	25	24	457.4692	10	91	90	475.7114	1
65	66	415.2345	16	26	25	457.8286	17	92	91	475.8986	-8
63	64	416.3550	15	27	26	458.1829	-3	93	92	476.0837	-10
62	63	416.9110	2	28	27	458.5369	-0	94	93	476.2675	2
61	62	417.4663	3	29	28	458.8889	6	95	94	476.4480	9
60	61	418.0194	2	30	29	459.2378	6	96	95	476.6259	18
59	60	418.5705	2	31	30	459.5864	27	97	96	476.7985	1
57	58	419.6673	9	32	31	459.9284	6	98	97	476.9697	-1
56	57	420.2127	14	33	32	460.2693	-1	99	98	477.1389	3
55	56	420.7540	-1	34	33	460.6086	1	100	99	477.3045	0
54	55	421.2949	-1	35	34	460.9449	-2	101	100	477.4679	3
53	54	421.8329	-8	36	35	461.2791	-2	102	101	477.6281	1
52	53	422.3722	19	37	36	461.6107	-3	103	102	477.7864	9
51	52	422.9038	-12	38	37	461.9400	-2	104	103	477.9400	-2
50	51	423.4370	-4	39	38	462.2665	-4	105	104	478.0922	1

clearly visible. Figure 2 shows a portion of the spectrum near the 4–3 bandhead with the rotational assignments for ^{138}BaF. The rotational assignments were made by predicting the vibration–rotation band line positions using the rotational and vibrational constants (*10*). The line positions were then fitted to the energy level expression (*21*)

$$F_{v,N} = T_v + B_vN(N + 1) - D_v[N(N + 1)]^2. \quad (1)$$

The spin–rotation coupling terms were not included in the fit because the spin–rotation splitting was not resolved in this experiment. After the preliminary constants

TABLE Ia—*Continued*

N'	N''	ν_{obs}	10^4O-C	N'	N''	ν_{obs}	10^4O-C	N'	N''	ν_{obs}	10^4O-C
106	105	478.2410	-3	34	33	456.9851	-2	101	100	473.7049	18
107	106	478.3878	2	35	34	457.3199	2	102	101	473.8612	-3
108	107	478.5302	-8	36	35	457.6496	-21	103	102	474.0165	-5
110	109	478.8091	-5	37	36	457.9793	-19	104	103	474.1726	28
111	110	478.9459	14	38	37	458.3082	1	105	104	474.3183	-15
112	111	479.0742	-24	39	38	458.6327	-0	106	105	474.4683	14
113	112	479.2063	4	40	39	458.9547	0	107	106	474.6084	-28
	7 - 6 band			41	40	459.2712	-31	108	107	474.7537	10
58	59	415.7140	-8	42	41	459.5864	-48	109	108	474.8910	-5
57	58	416.2601	7	43	42	459.9055	-3	110	109	475.0274	1
56	57	416.8021	3	44	43	460.2180	1	111	110	475.1606	2
55	56	417.3447	26	45	44	460.5275	2	114	113	475.5400	-23
54	55	417.8791	-14	46	45	460.8340	-3	115	114	475.6641	1
53	54	418.4186	19	47	46	461.1392	3	117	116	475.8986	-0
52	53	418.9501	-8	49	48	461.7392	-10	118	117	476.0113	-4
49	50	420.5397	-11	50	49	462.0376	5	120	119	476.2283	-8
47	48	421.5902	-1	51	50	462.3311	-3	122	121	476.4349	-2
46	47	422.1122	3	52	51	462.6237	5	123	122	476.5367	30
45	46	422.6333	18	53	52	462.9124	-1	125	124	476.7228	7
44	45	423.1492	3	54	53	463.1996	4	127	126	476.8993	3
43	44	423.6638	-4	55	54	463.4836	3	128	127	476.9823	-8
42	43	424.1774	1	56	55	463.7654	6	131	130	477.2166	-11
41	42	424.6881	-3	57	56	464.0429	-10	132	131	477.2918	18
40	41	425.1948	-25	58	57	464.3200	-3	133	132	477.3602	9
37	38	426.7111	-1	59	58	464.5919	-22	134	133	477.4255	-3
36	37	427.2120	4	60	59	464.8660	6	136	135	477.5491	-5
35	36	427.7092	-5	61	60	465.1328	-13	138	137	477.6632	15
34	35	428.2038	-21	62	61	465.3979	-23	139	138	477.7131	-2
33	34	428.6993	-4	63	62	465.6635	-2	140	139	477.7629	11
32	33	429.1904	-11	64	63	465.9220	-25	143	142	477.8900	4
31	32	429.6807	-4	65	64	466.1828	-1	145	144	477.9591	-7
30	31	430.1686	1	66	65	466.4375	-10	146	145	477.9904	0
28	29	431.1372	4	67	66	466.6921	6	147	146	478.0167	-12
27	28	431.6181	5	68	67	466.9418	-2		**8 - 7 band**		
26	27	432.0970	7	69	68	467.1899	2	56	57	413.4140	21
25	26	432.5731	4	70	69	467.4355	5	51	52	416.0804	-2
24	25	433.0474	3	71	70	467.6771	-4	50	51	416.6111	30
23	24	433.5235	43	72	71	467.9126	-47	49	50	417.1335	-1
22	23	433.9917	27	73	72	468.1536	-10	47	48	418.1778	-4
21	22	434.4562	-6	74	73	468.3927	35	44	45	419.7278	-14
20	21	434.9204	-19	75	74	468.6207	-5	42	43	420.7540	13
19	20	435.3865	10	76	75	468.8513	9	41	42	421.2596	-18
18	19	435.8441	-25	77	76	469.0736	-34	40	41	421.7657	-21
17	18	436.3054	1	78	77	469.3022	13	38	39	422.7740	-4
16	17	436.7618	-1	79	78	469.5234	12	36	37	423.7700	-23
15	16	437.2176	14	80	79	469.7408	1	35	36	424.2687	6
12	13	438.5671	14	81	80	469.9573	6	34	35	424.7635	17
14	13	449.7860	8	82	81	470.1712	13	33	34	425.2540	7
15	14	450.1675	-5	83	82	470.3843	39	30	31	426.7111	-36
16	15	450.5486	1	84	83	470.5895	13	29	30	427.2017	42
17	16	450.9275	8	85	84	470.7926	-8	28	29	427.6793	11
18	17	451.2989	-35	86	85	470.9968	11	27	28	428.1562	-5
19	18	451.6762	6	87	86	471.1960	6	26	27	428.6336	6
21	20	452.4152	1	88	87	471.3943	20	25	26	429.1060	-11
22	21	452.7806	-6	89	88	471.5862	-4	24	25	429.5816	26
23	22	453.1449	1	90	89	471.7774	-7	23	24	430.0469	-18
24	23	453.5055	-7	91	90	471.9686	17	22	23	430.5174	12
25	24	453.8646	-4	92	91	472.1529	-0	21	22	430.9818	3
26	25	454.2185	-30	93	92	472.3348	-14	17	18	432.8226	21
27	26	454.5752	-3	94	93	472.5173	6	16	17	433.2750	2
28	27	454.9272	1	95	94	472.6939	-6	14	15	434.1754	-11
29	28	455.2770	8	96	95	472.8687	-8	12	11	445.4578	-2
30	29	455.6232	2	97	96	473.0416	-2	13	12	445.8426	-8
31	30	455.9695	23	98	97	473.2105	-8	14	13	446.2236	-27
32	31	456.3095	4	99	98	473.3737	-43	20	19	448.4752	10
33	32	456.6484	-0	100	99	473.5422	3	21	20	448.8391	-13

were derived, we predicted the higher vibrational bands and assigned the lines using the Loomis–Wood program. The minor isotopomer line positions were predicted by using the constants of ^{138}BaF and the mass relations, and they were also assigned with the help of the Loomis–Wood program. In total, about 1750 lines for ^{138}BaF, about 270 lines for ^{137}BaF, and about 70 lines for ^{136}BaF were assigned. Table I lists all of our assigned infrared vibration–rotation transitions, along with the pure rotational transitions (corrected for the effects of fine structure and hyperfine structure) taken from Refs. (*10, 11*).

TABLE Ia—*Continued*

N'	N''	ν_{obs}	10^4O-C	N'	N''	ν_{obs}	10^4O-C	N'	N''	ν_{obs}	10^4O-C
22	21	449.2053	9	89	88	467.8695	23	47	46	453.8958	7
23	22	449.5651	-7	90	89	468.0556	-11	48	47	454.1933	6
24	23	449.9261	13	91	90	468.2431	-4	49	48	454.4881	2
25	24	450.2811	-4	92	91	468.4282	7	50	49	454.7808	4
26	25	450.6348	-9	93	92	468.6071	-17	51	50	455.0705	0
27	26	450.9876	1	94	93	468.7878	4	52	51	455.3587	6
28	27	451.3362	-6	95	94	468.9628	-4	53	52	455.6404	-26
29	28	451.6839	1	96	95	469.1359	-3	54	53	455.9263	8
30	29	452.0291	9	97	96	469.3022	-44	55	54	456.2048	-6
31	30	452.3695	-8	98	97	469.4722	-19	56	55	456.4814	-13
32	31	452.7104	5	99	98	469.6394	5	57	56	456.7582	8
33	32	453.0472	1	100	99	469.8008	-1	58	57	457.0294	-2
34	33	453.3822	5	101	100	469.9573	-28	59	58	457.3003	11
35	34	453.7133	-7	102	101	470.1161	-4	60	59	457.5668	5
36	35	454.0434	-4	104	103	470.4206	-4	61	60	457.8286	-21
37	36	454.3713	3	105	104	470.5720	30	62	61	458.0914	-12
38	37	454.6958	-1	106	105	470.7140	-2	63	62	458.3521	2
39	38	455.0178	-4	107	106	470.8573	6	64	63	458.6075	-11
40	39	455.3386	6	108	107	470.9968	5	65	64	458.8630	3
41	40	455.6554	1	116	115	472.0101	-11	66	65	459.1136	-6
42	41	455.9695	-7	117	116	472.1264	12	67	66	459.3634	4
43	42	456.2822	-4	118	117	472.2358	-7	68	67	459.6086	-7
44	43	456.5924	-1	122	121	472.6518	-6	69	68	459.8531	2
45	44	456.8993	-5	125	124	472.9353	11	70	69	460.0945	5
46	45	457.2039	-7			**9 - 8 band**		71	70	460.3328	4
47	46	457.5077	8	54	55	411.1111	5	72	71	460.5690	9
48	47	457.8062	-6	49	50	413.7460	-1	73	72	460.8041	29
49	48	458.1039	-1	44	45	416.3289	-5	74	73	461.0345	28
50	49	458.3992	5	42	43	417.3447	-32	76	75	461.4835	-12
51	50	458.6900	-9	38	39	419.3602	5	77	76	461.7062	-11
52	51	458.9803	-2	36	37	420.3543	14	78	77	461.9280	9
53	52	459.2712	35	34	35	421.3359	-15	79	78	462.1435	-7
54	53	459.5533	10	33	34	421.8236	-29	81	80	462.5723	17
55	54	459.8346	3	31	32	422.7979	-2	82	81	462.7797	-1
56	55	460.1129	-8	29	30	423.7582	-30	83	82	462.9871	9
57	56	460.3913	7	28	29	424.2391	-3	84	83	463.1905	5
58	57	460.6659	10	16	17	429.8066	-7	85	84	463.3901	-10
59	58	460.9339	-26	10	11	432.4725	10	86	85	463.5893	-2
60	59	461.2054	-4	5	6	434.6298	2	87	86	463.7871	20
61	60	461.4728	5	16	15	443.4421	5	88	87	463.9780	-1
62	61	461.7392	29	18	17	444.1867	3	91	90	464.5402	-5
63	62	461.9981	5	19	18	444.5573	21	92	91	464.7243	15
64	63	462.2566	2	20	19	444.9206	-10	93	92	464.9021	-0
65	64	462.5175	49	21	20	445.2859	3	94	93	465.0773	-14
66	65	462.7673	11	22	21	445.6455	-18	97	96	465.5915	-4
67	66	463.0162	-10	23	22	446.0073	8	99	98	465.9220	17
68	67	463.2665	10	24	23	446.3664	31	101	100	466.2380	3
69	68	463.5115	4	25	24	446.7174	-4	102	101	466.3930	9
70	69	463.7534	-8	26	25	447.0718	20	103	102	466.5430	-9
71	70	463.9985	38	27	26	447.4184	-9	104	103	466.6921	-7
72	71	464.2325	-1	28	27	447.7665	1	106	105	466.9827	5
73	72	464.4675	-2	29	28	448.1091	-21	107	106	467.1206	-22
74	73	464.7006	4	30	29	448.4542	7	108	107	467.2614	10
75	74	464.9281	-20	31	30	448.7919	-15	109	108	467.3938	-15
76	75	465.1567	-6	32	31	449.1305	-2	110	109	467.5284	10
77	76	465.3829	10	33	32	449.4674	17	111	110	467.6567	1
78	77	465.6028	-10	34	33	449.7986	4	112	111	467.7831	1
80	79	466.0401	6	36	35	450.4572	15	114	113	468.0272	-1
81	80	466.2488	-46	37	36	450.7799	-9	118	117	468.4807	-12
82	81	466.4647	2	38	37	451.1034	-1	122	121	468.8922	17
83	82	466.6734	3	39	38	451.4237	0	123	122	468.9870	15
84	83	466.8770	-18	42	41	452.3695	4	125	124	469.1660	-7
85	84	467.0819	-1	43	42	452.6803	10	126	125	469.2531	2
86	85	467.2829	6	44	43	452.9864	-7			**10 - 9 band**	
87	86	467.4778	-22	45	44	453.2911	-12	48	49	410.8984	13
88	87	467.6771	21	46	45	453.5946	-4	43	44	413.4554	-21

Once all of the lines were assigned, we fitted the line positions of each isotopomer in combination with the microwave data (*10, 11*) to Eq. (1) to obtain the rotational constants and the vibrational term energy. The rotational constants for the three most abundant isotopomers are listed in Table II. Although we have assigned rotational transitions involving the quantum number N up to nearly 150, higher order centrifugal distortion corrections, H_v, were not needed in the fit.

The line positions of each isotopomer were also fitted to the Dunham energy level expression (*22*)

TABLE Ia—*Continued*

N'	N''	ν_{obs}	10^4O-C	N'	N''	ν_{obs}	10^4O-C	N'	N''	ν_{obs}	10^4O-C
37	38	416.4605	3	80	79	458.7001	2	81	80	455.2658	-38
36	37	416.9485	-48	81	80	458.9075	-22	82	81	455.4727	-25
34	35	417.9320	-9	82	81	459.1136	-33	84	83	455.8789	7
33	34	418.4186	-10	85	84	459.7218	-5	85	84	456.0722	-37
27	28	421.2949	10	86	85	459.9156	-31	86	85	456.2676	-31
26	27	421.7657	4	87	86	460.1129	5	88	87	456.6484	-41
14	15	427.2497	-20	88	87	460.3045	11	90	89	457.0190	-46
13	14	427.6953	8	89	88	460.4915	-1	91	90	457.2039	-12
12	13	428.1356	6	90	89	460.6768	-5	92	91	457.3848	8
12	11	438.4079	-7	93	92	461.2157	-19	94	93	457.7336	1
14	13	439.1682	3	94	93	461.3931	9			**12 - 11 band**	
17	16	440.2885	-5	97	96	461.8997	-1	3	2	427.9451	-36
19	18	441.0271	25	99	98	462.2219	-23	7	6	429.5240	1
24	23	442.8221	4	103	102	462.8390	-12	8	7	429.9133	14
26	25	443.5243	7	104	103	462.9871	-0	13	12	431.8135	-32
28	27	444.2181	21	105	104	463.1315	2	16	15	432.9321	5
29	28	444.5573	-13	107	106	463.4112	-2	21	20	434.7426	5
32	31	445.5701	-15	108	107	463.5484	12	22	21	435.0975	3
33	32	445.9043	0	109	108	463.6815	13	25	24	436.1466	-11
35	34	446.5652	27	110	109	463.8091	-13	26	25	436.4955	24
36	35	446.8880	1	112	111	464.0626	3	27	26	436.8337	-24
38	37	447.5308	-5	115	114	464.4190	1	28	27	437.1717	-49
39	38	447.8480	-14			**11 - 10 band**		33	32	438.8359	-71
40	39	448.1656	7	22	21	438.5992	12	34	33	439.1682	-8
41	40	448.4752	-28	29	28	441.0271	-29	35	34	439.4921	-5
42	41	448.7919	34	33	32	442.3616	-48	36	35	439.8090	-46
43	42	449.0986	21	38	37	443.9799	-17	39	38	440.7627	6
44	43	449.4015	-6	39	38	444.2960	-13	40	39	441.0760	27
45	44	449.7042	-10	40	39	444.6062	-42	44	43	442.3008	75
46	45	450.0085	27	41	40	444.9206	-6	47	46	443.1816	-6
47	46	450.3037	-1	42	41	445.2320	26	48	47	443.4722	-13
48	47	450.6008	15	43	42	445.5356	5	50	49	444.0479	-7
49	48	450.8919	-5	44	43	445.8426	41	51	50	444.3346	23
50	49	451.1813	-15	45	44	446.1432	40	54	53	445.1660	-24
51	50	451.4713	5	46	45	446.4357	-18	55	54	445.4422	2
52	51	451.7561	-1	47	46	446.7272	-60	56	55	445.7172	41
53	52	452.0408	17	48	47	447.0278	13	59	58	446.5138	29
54	53	452.3201	7	49	48	447.3159	-13	60	59	446.7715	-3
55	54	452.6001	28	50	49	447.6071	17	61	60	447.0278	-23
56	55	452.8725	-0	51	50	447.8905	-6	62	61	447.2860	3
57	56	453.1449	-2	52	51	448.1767	25	64	63	447.7887	-8
58	57	453.4156	3	53	52	448.4542	-7	65	64	448.0354	-20
59	58	453.6834	6	54	53	448.7361	30	66	65	448.2828	1
60	59	453.9459	-19	55	54	449.0082	-4	68	67	448.7660	4
62	61	454.4703	3	56	55	449.2772	-45	69	68	449.0082	50
64	63	454.9841	22	57	56	449.5525	3	70	69	449.2407	26
65	64	455.2334	-5	58	57	449.8203	3	72	71	449.7042	40
66	65	455.4832	-2	59	58	450.0866	11	73	72	449.9261	-11
67	66	455.7297	-5	60	59	450.3494	10	79	78	451.2343	-1
69	68	456.2160	-1	62	61	450.8686	24	81	80	451.6443	-45
70	69	456.4558	8	65	64	451.6264	25	82	81	451.8527	6
71	70	456.6935	21	66	65	451.8738	24	83	82	452.0529	2
72	71	456.9258	6	68	67	452.3588	4	84	83	452.2493	-13
73	72	457.1584	21	69	68	452.6001	21	89	88	453.2004	8
74	73	457.3848	0	71	70	453.0690	-5	90	89	453.3822	8
75	74	457.6094	-12	73	72	453.5309	5	91	90	453.5610	6
77	76	458.0543	1	74	73	453.7559	-12	92	91	453.7355	-12
78	77	458.2714	-7	75	74	453.9823	13				
79	78	458.4867	-6	78	77	454.6364	-8				

* The $\Delta v = 0$ bands were derived from microwave data in ref[10].

$$F_{v,N} = \sum_{l,m} Y_{lm}\left(v + \frac{1}{2}\right)^l [N(N+1)]^m. \tag{2}$$

The Dunham coefficients are listed in Table III for each isotopomer. For convenience, we also list the spin–rotation constants from Refs. (*10, 11*). The Dunham coefficients are isotope dependent and vary approximately with powers of the reduced mass ratio μ/μ^i,

$$Y^i_{lm} = Y_{lm}\left(\frac{\mu}{\mu^i}\right)^{(l/2+m)}, \tag{3}$$

TABLE Ib

Line Positions of ^{137}BaF in cm^{-1}

N'	N"	ν_{obs}	10^4O-C	N'	N"	ν_{obs}	10^4O-C	N'	N"	ν_{obs}	10^4O-C
		0 - 0 band*		8	9	458.3521	5	90	89	490.9141	-2
8	7	3.45784158	-0.0005	5	6	459.6864	-35	91	90	491.1133	-1
22	21	9.50222941	0.0002	4	3	463.9985	-23	92	91	491.3068	-30
		1 - 0 band		5	4	464.4190	-0	93	92	491.5037	3
6	5	468.4994	36	14	13	468.0728	-44	94	93	491.6949	7
9	8	469.7408	46	15	14	468.4736	18			**3 - 2 band**	
11	10	470.5518	4	16	15	468.8636	-4	25	24	468.6071	50
12	11	470.9578	25	17	16	469.2531	-7	26	25	468.9746	68
13	12	471.3568	-2	18	17	469.6394	-18	30	29	470.4073	10
14	13	471.7581	20	20	19	470.4073	-15	31	30	470.7589	-8
15	14	472.1529	-1	21	20	470.7926	37	34	33	471.8050	-2
22	21	474.8570	-62	22	21	471.1658	-9	36	35	472.4901	2
23	22	475.2358	-49	26	25	472.6518	-14	37	36	472.8288	3
25	24	475.9857	-27	27	26	473.0191	3	42	41	474.4825	-15
27	26	476.7228	-35	29	28	473.7427	2	43	42	474.8105	29
28	27	477.0920	4	30	29	474.1012	4	44	43	475.1310	24
31	30	478.1717	-10	32	31	474.8105	7	45	44	475.4474	2
33	32	478.8788	-23	33	32	475.1606	-0	46	45	475.7633	1
35	34	479.5772	-25	34	33	475.5095	6	48	47	476.3877	2
36	35	479.9217	-34	36	35	476.1984	3	49	48	476.6947	-12
38	37	480.6108	21	37	36	476.5367	-23	50	49	476.9999	-18
39	38	480.9475	8	38	37	476.8781	8	51	50	477.3045	-4
40	39	481.2809	-14	39	38	477.2166	33	52	51	477.6028	-28
41	40	481.6146	-7	40	39	477.5491	25	53	52	477.9020	-18
42	41	481.9461	2	41	40	477.8762	-12	54	53	478.2022	29
45	44	482.9244	20	42	41	478.2022	-36	55	54	478.4926	3
46	45	483.2441	12	43	42	478.5302	-14	56	55	478.7787	-40
47	46	483.5618	10	44	43	478.8561	12	59	58	479.6385	0
49	48	484.1935	45	45	44	479.1754	-3	60	59	479.9217	32
50	49	484.4988	-6	46	45	479.4935	-4	61	60	480.1958	-2
51	50	484.8051	-20	47	46	479.8088	-8	62	61	480.4693	-15
52	51	485.1137	14	49	48	480.4352	19	63	62	480.7431	1
53	52	485.4130	-20	50	49	480.7431	17	64	63	481.0115	-12
54	53	485.7143	-8	51	50	481.0463	-6	65	64	481.2809	13
57	56	486.6006	6	52	51	481.3485	-14	66	65	481.5434	-6
58	57	486.8906	8	53	52	481.6498	-5	67	66	481.8064	7
59	58	487.1777	7	54	53	481.9461	-19	69	68	482.3190	-23
60	59	487.4659	41	55	54	482.2456	24	70	69	482.5726	-25
62	61	488.0195	-39	56	55	482.5387	28	71	70	482.8254	-8
63	62	488.3007	5	57	56	482.8254	-5	72	71	483.0753	6
69	68	489.9083	14	58	57	483.1136	3	73	72	483.3207	2
72	71	490.6727	-22	61	60	483.9606	5	74	73	483.5618	-20
74	73	491.1692	-45	62	61	484.2350	-22	75	74	483.8053	11
76	75	491.6608	-12	63	62	484.5108	-8	76	75	484.0430	10
		2 - 1 band		64	63	484.7839	4	77	76	484.2810	38
56	57	434.2203	17	65	64	485.0571	45	78	77	484.5108	11
53	54	435.8716	-9	66	65	485.3193	1	79	78	484.7396	2
48	49	438.5909	41	67	66	485.5831	1	82	81	485.4130	4
44	45	440.7205	4	68	67	485.8439	-5	83	82	485.6278	-37
41	42	442.3008	31	69	68	486.1011	-19	84	83	485.8526	49
40	41	442.8221	28	70	69	486.3607	17	85	84	486.0668	55
39	40	443.3366	-22	71	70	486.6122	-1	87	86	486.4807	6
38	39	443.8583	23	73	72	487.1104	-5	88	87	486.6856	1
37	38	444.3714	3	75	74	487.5984	-5	89	88	486.8906	26
34	35	445.9043	9	76	75	487.8389	-0	90	89	487.0874	-5
33	34	446.4106	7	77	76	488.0779	17	94	93	487.8564	-33
31	32	447.4184	22	78	77	488.3138	31	95	94	488.0462	4
30	31	447.9150	-12	79	78	488.5430	3	96	95	488.2300	10
28	29	448.9093	-1	80	79	488.7688	-31	97	96	488.4069	-26
27	28	449.4015	-12	81	80	489.0003	19	98	97	488.5853	-19
25	26	450.3836	10	82	81	489.2227	5	99	98	488.7586	-35
24	25	450.8686	-7	83	82	489.4410	-22	106	105	489.9083	5
23	24	451.3549	11	85	84	489.8794	22	107	106	490.0595	-7
15	16	455.1510	19	87	86	490.3002	-1	109	108	490.3562	-4
12	13	456.5353	1	88	87	490.5074	-2				

* The $\Delta v = 0$ bands were derived from microwave data in ref[11].

where the *i* designates an isotopic species. Finally, all of the assigned infrared vibration–rotation transitions and the microwave pure rotation lines (*10, 11*) were fitted to the mass-reduced Dunham expression

$$F_{v,N} = \sum_{l,m} \mu^{-(l/2+m)} U_{lm} \left(v + \frac{1}{2} \right)^l [N(N+1)]^m, \qquad (4)$$

TABLE Ib—*Continued*

N'	N"	ν_{obs}	10^4O-C	N'	N"	ν_{obs}	10^4O-C	N'	N"	ν_{obs}	10^4O-C
		4 - 3 band		61	60	476.4480	-23			**5 - 4 band**	
26	25	465.2993	-7	62	61	476.7228	-2	30	29	463.0831	21
27	26	465.6635	26	63	62	476.9999	69	31	30	463.4321	26
28	27	466.0139	-56	64	63	477.2607	2	36	35	465.1328	-21
30	29	466.7293	-0	65	64	477.5233	-20	39	38	466.1275	-9
31	30	467.0755	-50	66	65	477.7864	-11	40	39	466.4517	-30
34	33	468.1234	41	67	66	478.0454	-18	41	40	466.7761	-23
35	34	468.4623	17	68	67	478.3047	6	42	41	467.0979	-17
37	36	469.1359	1	69	68	478.5590	5	46	45	468.3569	-26
38	37	469.4722	25	70	69	478.8091	-10	47	46	468.6691	9
39	38	469.8008	-3	74	73	479.7902	-1	48	47	468.9746	3
40	39	470.1309	10	75	74	480.0311	24	50	49	469.5808	16
44	43	471.4206	3	77	76	480.4975	1	51	50	469.8740	-38
45	44	471.7369	3	78	77	480.7307	29	52	51	470.1712	-28
46	45	472.0500	-3	79	78	480.9576	21	53	52	470.4684	9
47	46	472.3613	-3	80	79	481.1800	-5	54	53	470.7589	3
48	47	472.6643	-60	81	80	481.3997	-31	55	54	471.0482	11
49	48	472.9780	16	82	81	481.6238	14	56	55	471.3333	2
50	49	473.2870	69	83	82	481.8395	2	58	57	471.8970	-5
51	50	473.5832	21	84	83	482.0496	-38	61	60	472.7269	19
52	51	473.8787	-9	87	86	482.6833	36	62	61	472.9985	28
53	52	474.1726	-30	88	87	482.8833	4	63	62	473.2660	21
54	53	474.4683	-6	90	89	483.2816	3	64	63	473.5316	20
55	54	474.7537	-60	91	90	483.4768	4	65	64	473.7932	6
56	55	475.0479	-0	94	93	484.0430	-20	67	66	474.3097	-14
58	57	475.6169	3	95	94	484.2268	-23	70	69	475.0686	-10
59	58	475.8986	15	96	95	484.4097	-6				
60	59	476.1748	-3	97	96	484.5891	2				

where U_{lm} are the mass-reduced Dunham constants. The mass-reduced Dunham constants are listed in Table IV.

An unsuccessful attempt was made to estimate the Born–Oppenheimer breakdown constants Δ_{lm}^{Ba} (*23, 24*) using

TABLE Ic

Line Positions of ^{136}BaF in cm^{-1}

N'	N"	ν_{obs}	10^4O-C	N'	N	ν_{obs}	10^4O-C	N'	N"	ν_{obs}	10^4O-C
		0 - 0 band*		55	54	482.4649	22	53	52	478.1197	19
7	6	3.0283979	-0.0019	56	55	482.7563	7	59	58	479.8535	4
21	20	9.0791038	0.0063	57	56	483.0462	2	60	59	480.1366	32
22	21	9.5107409	-0.0054	58	57	483.3342	5	62	61	480.6868	8
		1 - 0 band		62	61	484.4587	-1	63	62	480.9576	-9
44	43	482.8233	69	63	62	484.7314	-23	65	64	481.4963	6
45	44	483.1412	2	65	64	485.2745	-9	66	65	481.7591	-13
46	45	483.4610	-17	66	65	485.5430	6	69	68	482.5387	-2
47	46	483.7816	3	68	67	486.0668	-16	71	70	483.0462	14
49	48	484.4077	-18	70	69	486.5841	1	73	72	483.5408	5
50	49	484.7193	4	72	71	487.0874	-17	74	73	483.7837	-5
51	50	485.0291	40	74	73	487.5831	-6	77	76	484.4988	-12
		2 - 1 band		75	74	487.8268	-1	78	77	484.7314	-19
20	19	470.6177	3	86	85	490.3295	15	82	81	485.6383	-21
28	27	473.5943	4			**3 - 2 band**		85	84	486.2933	4
38	37	477.0920	-5	25	24	468.8155	12	86	85	486.5072	20
39	38	477.4255	-32	26	25	469.1806	4	91	90	487.5355	87
40	39	477.7629	7	29	28	470.2621	-11			**4 - 3 band**	
41	40	478.0922	-12	30	29	470.6177	-16	60	59	476.3877	-1
42	41	478.4208	-12	31	30	470.9704	-25	61	60	476.6643	7
43	42	478.7475	-6	35	34	472.3613	-11	62	61	476.9363	-3
44	43	479.0742	25	37	36	473.0416	-5	63	62	477.2050	-21
46	45	479.7119	7	41	40	474.3708	-10	65	64	477.7398	-5
48	47	480.3407	2	45	44	475.6641	31	66	65	478.0039	11
50	49	480.9576	-20	46	45	475.9769	-1	67	66	478.2633	5
51	50	481.2660	6	48	47	476.6034	21	68	67	478.5194	-7
53	52	481.8690	-2	49	48	476.9105	7				
54	53	482.1685	12	50	49	477.2166	9				

* The $\Delta v = 0$ bands were derived from microwave data in ref[10].

TABLE II

Molecular Constants for BaF in cm^{-1}*

v	T_v	B_v	$10^7 D_v$
		^{138}BaF	
0	0.0	0.215948014(12)	1.84452(13)
1	465.745446(66)	0.214785499(12)	1.84763(12)
2	927.848552(98)	0.213624003(18)	1.85062(12)
3	1386.32832(12)	0.212463601(20)	1.85349(11)
4	1841.20379(13)	0.211304322(22)	1.85615(11)
5	2292.49399(17)	0.210146421(44)	1.85874(11)
6	2740.21828(21)	0.208989952(77)	1.86122(12)
7	3184.39636(24)	0.207834876(85)	1.86351(12)
8	3625.04762(28)	0.206681346(103)	1.86560(12)
9	4062.19176(32)	0.20552947(12)	1.86755(13)
10	4495.84828(38)	0.20437968(15)	1.86951(14)
11	4926.04426(84)	0.20322805(37)	1.86709(36)
12	5352.78736(90)	0.20208180(42)	1.86867(42)
		^{137}BaF	
0	0.0	0.216138773(31)	1.84932(34)
1	465.95131(41)	0.21497196(28)	1.84624(50)
2	928.25559(48)	0.21380895(32)	1.84946(52)
3	1386.93445(73)	0.21264665(38)	1.85215(53)
4	1842.00509(96)	0.21148539(46)	1.85438(58)
5	2293.5045(21)	0.2103147(15)	1.8402(24)
		^{136}BaF	
0	0.0	0.216332277(34)	1.84982(38)
1	466.009(38)	0.215293(33)	2.127(70)
2	928.511(39)	0.214128(33)	2.117(68)
3	1387.391(41)	0.212959(33)	2.103(65)
4	1842.632(74)	0.211804(44)	2.104(72)

* One standard deviation error is provided in parentheses.

$$Y_{lm} = \mu^{-(l/2+m)} U_{lm} \left[1 + \left(\frac{m_e}{M_{\mathrm{Ba}}} \right) \Delta_{lm}^{\mathrm{Ba}} \right], \tag{5}$$

where m_e and M_{Ba} are electron mass and atomic mass of barium. This means that Born–Oppenheimer breakdown is negligible for the heavy barium atom.

CONCLUSION

Fourier transform infrared emission spectroscopy is a very powerful technique for the study of high-temperature free radicals. It has been shown that this technique covers a wide spectral range and provides a large number of line positions with high precision. Our infrared vibration–rotational data of the three most abundant isotopomers, ^{138}BaF, ^{137}BaF, and ^{136}BaF, together with the microwave data in the literature (*10, 11*) were used to derive a set of improved spectroscopic constants.

TABLE III

Dunham Coefficients of BaF in cm^{-1}

	^{138}BaF	^{137}BaF	^{136}BaF
Y_{01}	0.216529618(17)[a]	0.216721093(64)	0.216915120(59)
10^7 Y_{02}	-1.84291(14)	-1.84777(39)	-1.84818(40)
Y_{10}	469.40570(13)	469.61261(61)	469.81386(112)
10^3 Y_{11}	-1.163429(16)	-1.16485(12)	-1.16591(103)
10^{10} Y_{12}	-3.2567(93)	-3.064(100)	-3.271[b]
Y_{20}	-1.835197(48)	-1.83664(24)	-1.8353(45)
10^7 Y_{21}	4.346(64)	4.01(22)	4.361[b]
10^{12} Y_{22}	6.89(12)	6.90[b]	6.92[b]
10^3 Y_{30}	3.1057(64)	3.094(31)	2.704(56)
10^8 Y_{31}	1.432(97)	1.436[b]	1.439[b]
10^6 Y_{40}	5.62(27)	5.63[b]	5.64[b]
10^{10} Y_{41}	1.27(45)	1.27[b]	-
10^3 $\gamma_e^{(SR)}$	2.7013(6)[c]	2.7027(73)[d]	2.7069(14)[c]
10^6 α_γ	1.95(24)[c]	-	1.95(24)[c]
10^6 δ_γ	3.74(57)[c]	3.77(490)[d]	3.74(57)[c]

a) One standard deviation error is provided in parenthesis.
b) The values were calculated using the ^{138}BaF constants and the mass relations and were fixed in the fit.
c) Ref[10].
d) Ref[11].

TABLE IV

Mass-Reduced Dunham Coefficients for BaF in cm^{-1}*

U_{01}	3.61561447(48)
10^5 U_{02}	-5.1387(70)
U_{10}	1918.14144(86)
10^2 U_{11}	-7.93826(16)
10^7 U_{12}	-3.705(19)
U_{20}	-30.643(12)
10^4 U_{21}	1.1709(16)
10^8 U_{22}	3.1718(95)
U_{30}	0.21121(59)
10^5 U_{31}	1.9182(38)
10^3 U_{40}	1.697(97)
$m_{Ba}(^{138}Ba)$/amu	137.905232
$m_{Ba}(^{137}Ba)$/amu	136.905812
$m_{Ba}(^{136}Ba)$/amu	135.904553
m_F/amu	18.99840322

* One standard deviation error is provided in parentheses.

ACKNOWLEDGMENT

The authors thank the Natural Science and Engineering Research Council of Canada (NSERC) for support of this research.

RECEIVED: August 30, 1994

REFERENCES

1. A. MITSCHERLICH, *Poggendorffs Ann.* **121,** 459–488 (1864).
2. H. GEORGE, *Z. Wiss. Photogr.* **12,** 237–243 (1913).
3. S. DATTA, *Proc. R. Soc. London A* **99,** 436–455 (1921).
4. R. C. JOHNSON, *Proc. R. Soc. London A* **122,** 189–200 (1929).
5. T. E. NEVIN, *Proc. Phys. Soc.* **43,** 554–558 (1931).
6. O. H. WALTERS AND S. BARRATT, *Proc. R. Soc. London A* **118,** 120–137 (1928).
7. F. A. JENKINS AND A. HARVEY, *Phys. Rev.* **39,** 922–931 (1932).
8. R. F. BARROW, M. W. BASTIN, AND B. LONGBOROUGH, *Proc. Phys. Soc.* **92,** 518–519 (1967).
9. J. SINGH AND H. MOHAN, *J. Phys. B* **4,** 1395–1397 (1971).
10. CH. RYZLEWICZ AND T. TÖRRING, *Chem. Phys.* **51,** 329–334 (1980).
11. CH. RYZLEWICZ, H.-U. SCHÜTZE-PAHLMANN, J. HOEFT, AND T. TÖRRING, *Chem. Phys.* **71,** 389–399 (1982).
12. P. C. F. IP, P. BERNATH, AND R. W. FIELD, *J. Mol. Spectrosc.* **89,** 53–61 (1981).
13. (a) C. EFFANTIN, A. BERNARD, J. D'INCAN, G. WANNOUS, J. VERGÈS, AND R. F. BARROW, *Mol. Phys.* **70,** 735–745 (1990); (b) **70,** 747–755 (1990).
14. A. BERNARD, C. EFFANTIN, E. ANDRIANAVALONA, J. VERGÈS, AND R. F. BARROW, *J. Mol. Spectrosc.* **152,** 174–178 (1992).
15. C. EFFANTIN, A. BERNARD, J. D'INCAN, E. ANDRIANAVALONA, AND R. F. BARROW, *J. Mol. Spectrosc.* **145,** 456–457 (1992).
16. Z. J. JAKUBEK, N. A. HARRIS, R. W. FIELD, J. A. GARDNER, AND E. MURAD, *J. Chem. Phys.* **100,** 622–626 (1993).
17. Z. J. JAKUBEK AND R. W. FIELD, *Phys. Rev. Lett.* **72,** 2167–2170 (1994).
18. I. MILLS, T. CVITAS, K. HOMANN, N. KALLAY, AND K. KUCHITSU, "IUPAC Quantities, Units and Symbols in Physical Chemistry," Blackwell Scientific, Oxford, UK, 1989.
19. H. G. HEDDERICH, M. DULICK, AND P. F. BERNATH, *J. Chem. Phys.* **99,** 8363–8370 (1993).
20. R. B. LEBLANC, J. B. WHITE, AND P. F. BERNATH, *J. Mol. Spectrosc.* **164,** 574–579 (1994).
21. C. H. TOWNES AND A. L. SCHAWLOW, "Microwave Spectroscopy," Dover, New York, 1975.
22. J. L. DUNHAM, *Phys. Rev.* **41,** 721–888 (1932).
23. J. K. G. WATSON, *J. Mol. Spectrosc.* **45,** 99–113 (1973).
24. J. K. G. WATSON, *J. Mol. Spectrosc.* **80,** 411–421 (1980).